

Cosmic chronometers, Pantheon+ supernovae, and quasars favor coasting cosmologies over the flat Λ CDM model

PETER RAFFAI ^{1,2} ADRIENN PATAKI ¹ REBEKA L. BÖTTGER ¹ ALEXANDRA KARSAI ¹ AND GERGELY DÁLYA ^{3,4}

¹*Institute of Physics and Astronomy, ELTE Eötvös Loránd University, 1117 Budapest, Hungary*

²*HUN-REN-ELTE Extragalactic Astrophysics Research Group, 1117 Budapest, Hungary*

³*L2IT, Laboratoire des 2 Infinis - Toulouse, Université de Toulouse, CNRS/IN2P3, UPS, F-31062 Toulouse Cedex 9, France*

⁴*Department of Physics and Astronomy, Universiteit Gent, B-9000 Ghent, Belgium*

ABSTRACT

We test and compare coasting cosmological models with curvature parameters $k = \{-1, 0, +1\}$ in $H_0^2 c^{-2}$ units and the flat Λ CDM model by fitting them to cosmic chronometers (CC), the Pantheon+ sample of type Ia supernovae (SNe), and standardized quasars (QSOs). We used the `emcee` code for fitting CC data, a custom Markov Chain Monte Carlo implementation for SNe and QSOs, and Anderson-Darling tests for normality on normalized residuals for model comparison. Best-fit parameters are presented, constrained by data within redshift ranges $z \leq 2$ for CCs, $z \leq 2.3$ for SNe, and $z \leq 7.54$ for QSOs. Coasting models, particularly the flat coasting model, are generally favored over the flat Λ CDM model. The overfitting of the flat Λ CDM model to Pantheon+ SNe and the large intrinsic scatter in QSO data suggest a need to refine error estimates in these datasets. We also highlight the seemingly fine-tuned nature of either the CC data or $\Omega_{m,0}$ in the flat Λ CDM model to an $H_1 = H_0$ coincidence when fitting $H(z) = H_1 z + H_0$, a natural feature of coasting models.

1. INTRODUCTION

Coasting cosmologies are a family of cosmological models in which the $a(t)$ scale factor grows linearly with cosmic time t (for a review, see Casado 2020). This family includes *strictly linear* models where $a(t) \propto t$ at all times, and *quasi-linear* models which propose an early universe evolution in accordance with the concordance model (i.e., Lambda Cold Dark Matter or Λ CDM, see Peebles & Ratra 2003 for a review), with a transition to linear expansion sometime after recombination. Variations within coasting cosmologies arise from differences in the underlying assumptions driving the linear expansion and the value of the k spatial curvature parameter they propose or allow. For instance, the earliest coasting model, developed by Arthur Milne in the 1930s (Milne 1935), exhibits dynamics akin to an empty universe with zero Λ cosmological constant and negative k . The $R_h = ct$ model (Melia 2007; Melia & Shevchuk 2012; Melia 2020a) and the eternal coasting model by John and Joseph (John & Joseph 1996, 2000), suggest $k = 0$ and $k = +1$, respectively, although they permit any k

value (see, e.g., John & Joseph 2000, 2023). The hyperconical universe model introduced by Monjo (Monjo 2017, 2024) proposes linear expansion with $k = +1$ (for a comprehensive review on coasting models, see Casado 2020).

Despite the preeminent explanatory power of the Λ CDM model, tensions between the locally measured Hubble constant (H_0 ; Riess 2020) and structure growth parameter (S_8 ; Di Valentino et al. 2021) and those derived from cosmic microwave background (CMB) observations using the Λ CDM model (Aghanim et al. 2020), as well as other anomalies (Perivolaropoulos & Skara 2022), suggests the necessity of exploring alternative cosmologies. Coasting models fit remarkably well to a broad range of cosmological datasets at low redshifts (see, e.g., Table 2 in Melia 2018 and references therein). Strictly linear models offer natural solutions to several theoretical challenges in the Λ CDM model, including the horizon, flatness, cosmological constant, synchronicity, cosmic coincidence, and cosmic age problems (see Casado 2020 for a review). The horizon and flatness problems are addressed within the Λ CDM framework through the theory of cosmic inflation (Guth 1981; Baumann 2009), and other issues listed may represent unlikely coincidences in the realizations of Λ CDM model parameters. Strictly linear models, however, face sig-

nificant challenges in explaining observed phenomena presumably set by pre-recombination physics, such as light element abundances inherited from primordial nucleosynthesis (Kaplighat et al. 1999; Sethi et al. 1999; Kaplighat et al. 2000; Lewis et al. 2016) and CMB anisotropies (see, e.g., Fujii 2020; Melia 2020b, 2022), both of which are well explained by the Λ CDM framework (Dodelson 2003). Quasi-linear coasting models (e.g., Kolb 1989) are identical to the Λ CDM model before recombination, and thus are free from these challenges.

In Raffai et al. (2024a) we used gravitational-wave standard sirens (Holz & Hughes 2005) observed in the first three observing runs (Abbott et al. 2023a) of the LIGO-Virgo-KAGRA detector network (Aasi et al. 2015; Acernese et al. 2015; Akutsu et al. 2021) to constrain H_0 for coasting cosmologies with three fixed values of $k = \{-1, 0, +1\}$ in $H_0^2 c^{-2}$ units, where c is the speed of light in vacuum. From a combined analysis of 46 dark sirens and a single bright siren (Abbott et al. 2023b), we obtained maximum posteriors and 68.3% highest density intervals of $H_0 = \{68.1_{-5.6}^{+8.5}, 67.5_{-5.2}^{+8.3}, 67.1_{-5.8}^{+6.6}\}$ km s $^{-1}$ Mpc $^{-1}$, respectively. Our results constrained coasting models in the redshift range of $z \lesssim 0.8$, concluding that, within the broad ranges of measurement and source population modeling uncertainties, the tested coasting models and the flat ($k = 0$) Λ CDM model fit equally well to the gravitational-wave detections.

In this paper, we test and constrain the coasting models with $k = \{-1, 0, +1\}$ in $H_0^2 c^{-2}$ units and the flat Λ CDM model using cosmic chronometers (CCs), type Ia supernovae (SNe Ia), and quasars (QSOs). In Raffai et al. (2024a) we introduced $H_0 = 62.41_{-2.96}^{+2.95}$ km s $^{-1}$ Mpc $^{-1}$ as a reference for coasting models regardless of their k , determined from CCs with the differential age method (Jimenez & Loeb 2002; Simon et al. 2005a). In Section 2, we describe the details of how we obtained this reference H_0 . In Section 3 and Section 4, we present test results for SNe and QSOs. We discuss our findings and draw conclusions in Section 5.

2. TESTS WITH COSMIC CHRONOMETERS

In most cosmologies, including the Λ CDM and coasting models, $a(t)$ can be expressed as a function of the cosmological redshift z of photons emitted by sources at cosmic time t as $a(z) = (1+z)^{-1}$. In coasting cosmologies, $a(t) = H_0 t$, and thus $H(t) \equiv \dot{a} a^{-1} = t^{-1}$ (where the overdot indicates a derivative with respect to t) and $H(z) = H_0 a^{-1} = H_0(1+z)$ in the t and z range where linear expansion is assumed. In contrast,

$$H(z) = H_0 \sqrt{\Omega_{m,0} (1+z)^3 + 1 - \Omega_{m,0}} \quad (1)$$

in the flat Λ CDM model, where $\Omega_{m,0}$ is the matter density parameter today, and the contribution of radiation to the total density is neglected. We can also derive $H(z) = -\dot{z}(1+z)^{-1}$ for all cosmologies that satisfy $a(z) = (1+z)^{-1}$. The differential age method (Jimenez & Loeb 2002; Simon et al. 2005a) takes advantage of the fact that \dot{z} at z can in practice be approximated as $\dot{z} \approx \Delta z \Delta t^{-1}$, where Δz and Δt are the redshift and age differences of, e.g., pairs of galaxies with redshifts around z . Passively evolving galaxies allow measuring their Δt age differences from observed differences in their stellar populations, from which $H(z)$ can be determined with uncertainties typically dominated by uncertainties of the Δt measurement. Such objects utilized in measuring $H(z)$ are usually referred to as *cosmic chronometers* (CCs).

Melia & Maier (2013) determined H_0 for coasting models with CCs by fitting $H(z) = H_0(1+z)$ to 19 $H(z)$ measurements from Simon et al. (2005b); Stern et al. (2010); Moresco et al. (2012), and obtained $H_0 = 63.2 \pm 1.6$ km s $^{-1}$ Mpc $^{-1}$ regardless of k . We updated their result by fitting the $H(z)$ formula in coasting models to the 32 $H(z)$ measurements (Simon et al. 2005b; Stern et al. 2010; Moresco et al. 2012; Zhang et al. 2014; Moresco 2015; Moresco et al. 2016; Ratsimbazafy et al. 2017; Borghi et al. 2022) summarized in Table 1 of Moresco et al. (2022) using the **emcee**¹ (Foreman-Mackey et al. 2013) Markov Chain Monte Carlo (MCMC) code with the full statistical and systematic covariance matrix of the data. For comparisons, we also determined the best-fit parameters for a flat Λ CDM and a two-parameter $H(z) = H_1 z + H_0$ model using the same data and code. We show the 32 CC data points with 1σ error bars in Figure 1, along with the best-fit coasting $H(z)$ line and a reference Λ CDM $H(z)$ curve we obtained with the Planck+BAO cosmological parameters from Aghanim et al. (2020). We present the best-fit parameters for the tested models in Table 1 as the medians of the parameter posteriors, with averaged 1σ errors.

The fitted models are linear in H_0 , but the flat Λ CDM model is nonlinear in $\Omega_{m,0}$. Applying priors or external calibrators in fitting often causes models to become nonlinear in their fit parameters (Andrae et al. 2010). For models that are nonlinear in one or more fit parameters, the numbers of degrees of freedom (and thus the reduced chi-squares) cannot be estimated reliably. Additionally, the uncertainty in χ^2 limits its applicability in model comparisons, especially when the number of data points

¹ <https://gitlab.com/mmoresco/CCcovariance>

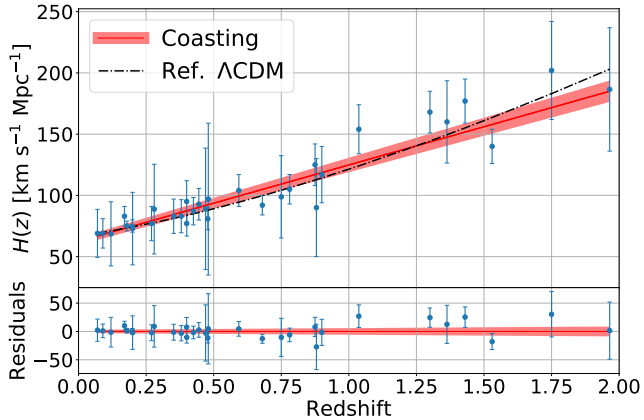


Figure 1. The 32 CC data points from Table 1 of Moresco et al. (2022) (blue dots with error bars), along with the best-fit coasting $H(z)$ (red solid) line plotted with 1σ confidence bands. For comparison, we also plotted the Λ CDM $H(z)$ curve with the Planck+BAO cosmological parameters from Aghanim et al. (2020) (upper panel, black dash-dotted curve). The lower panel shows the residuals after subtracting the best-fit coasting $H(z)$ line from the measured data points. Parameters of the coasting and reference Λ CDM models are given in Table 1.

is low (Andrae et al. 2010). Because of these considerations, following the recommendations in Andrae et al. (2010), we applied an Anderson-Darling (AD) test (Anderson & Darling 1952; The MathWorks Inc. 2024) to check if our normalized fit residuals follow a standard

Table 1. Model Fit and Test Results for CC Data

Fitted model	Best-fit parameters	χ^2	$\log_{10} p^{-1}$
Coasting	$H_0 = 62.41 \pm 2.96$	16.73	0.733*
$H_1 z + H_0$	$H_0 = 62.51 \pm 5.29$ $H_1 = 62.28 \pm 6.02$	16.73	
Flat Λ CDM	$H_0 = 66.70 \pm 5.41$ $\Omega_{m,0} = 0.33 \pm 0.07$	14.57	1.062*
Ref. Λ CDM	$H_0 = 67.66$ (fixed) $\Omega_{m,0} = 0.311$ (fixed)	14.62	

NOTE— $H_{\{0,1\}}$ values are given in $[\text{km s}^{-1} \text{Mpc}^{-1}]$ units. The fixed parameters of the reference Λ CDM model were taken from Aghanim et al. (2020). The χ^2 values were calculated with the `emcee` code (Foreman-Mackey et al. 2013) we used for model fitting. The p -values are results of the AD test we used for model testing. Asterisks mark models that are consistent with the null hypothesis of being the true model (i.e., $p \geq 0.05$ or $\log_{10} p^{-1} \leq 1.301$). We left the $\log_{10} p^{-1}$ column blank for the $H_1 z + H_0$ and Ref. Λ CDM models because we did not include them in the model comparison. Plots of posterior distributions are available in our public code repository (Raffai et al. 2024b).

normal distribution, which should be the case if a model is the true model underlying the data, and the data, after the necessary cleaning, preprocessing and error estimation procedure, is no longer contaminated with non-cosmological effects. We used the AD test p -values for model testing and $\log_{10} \mathcal{B} = \log_{10}(p_{\max}/p)$ Bayes factors for model comparisons, with p_{\max} as the highest p -value across all models, while retaining χ^2 -minimization for model fitting. We show the base 10 logs of the reciprocals of AD test p -values for the tested models in Table 1.

We have found no data points deviating by more than 3σ from the best-fit models or from the reference Λ CDM model. Models for which the AD test p -value is $p \geq 0.05$ ($\log_{10} p^{-1} \leq 1.301$) are considered consistent with the null hypothesis of being the true model. We found that all three coasting models and the flat Λ CDM model satisfy this condition, with the coasting models being slightly favored by the CC data ($\log_{10} \mathcal{B} = 0.329$), although the preference is not significant.

As Table 1 shows, the best-fit parameters for the flat Λ CDM model are consistent within 1σ with parameters of the reference Λ CDM model. For the $H(z) = H_1 z + H_0$ model, the best-fit H_0 and H_1 are equal to each other within $\sim 0.4\%$ and they match the best-fit H_0 for coasting models within $\sim 0.2\%$ (with χ^2 values matching to the given number of decimals). These results are curious given that (i) a flat Λ CDM universe does not imply the consistency of $H(z) = H_1 z + H_0$ with data extending to $z \gtrsim 1$, and (ii) even for $z \ll 1$, an effective H_1 in a flat Λ CDM universe depends on the unrelated values of H_0 and $\Omega_{m,0}$ ($H_1 = 3H_0\Omega_{m,0}/2$), which does not imply that the best-fit H_1 and H_0 should match. In contrast, these coincidences would be natural if the true cosmological model was a coasting one (at least in the $z \lesssim 2$ redshift range of the fitted CC data).

To evaluate the significance of the $H_1 = H_0$ coincidence, we kept the z redshifts and the $H(z)$ errors of the 32 actual CC measurements and simulated two sets of one million mock samples of 32 $H(z)$ measurements in Λ CDM universes described by Equation (1), with H_0 and $\Omega_{m,0}$ values randomized from normal distributions. The normal distributions in the first set were defined by the flat Λ CDM best-fit parameters in Table 1, and in the second set by the reference Λ CDM parameters $H_0 = 67.66 \pm 0.42 \text{ km s}^{-1} \text{ Mpc}^{-1}$ and $\Omega_{m,0} = 0.3111 \pm 0.0056$ from Aghanim et al. (2020). We fitted the $H_1 z + H_0$ model to the two sets and found that only 2% and 10% of the one million (H_1, H_0) pairs obtained from the fits were equal within 0.4% for the flat and reference Λ CDM models, respectively. We then created mock samples of 32 $H(z)$ measurements again

with the z and $H(z)$ errors of the real CC data, but calculated with fixed H_0 in Equation (1) and varied $\Omega_{m,0}$ over the interval $\Omega_{m,0} \in [0, 1.5]$. We found that regardless of what H_0 value we choose in Equation (1), only in the narrow interval of $\Omega_{m,0} \in [0.317, 0.320]$ do we get $H_1 = H_0$ coincidences within 0.4% precision, with the closest match at $\Omega_{m,0} = 0.3186$. Note that $\Omega_{m,0}$ in the reference Λ CDM model is consistent within $\sim 1\sigma$ with the narrow $\Omega_{m,0}$ interval corresponding to the $H_1 = H_0$ coincidence. This seemingly *fine-tuned* nature of either the CC data or $\Omega_{m,0}$ in the Λ CDM model to an $H_1 = H_0$ coincidence adds to the arguments for studying coasting models and makes our findings worth following up with an improved CC dataset in the future.

3. TESTS WITH TYPE IA SUPERNOVAE

We further tested and constrained the three coasting models and the flat Λ CDM model using the Pantheon+ sample of SNe Ia (Scolnic et al. 2022), compiled from 1701 light curves of 1550 SNe within $z \lesssim 2.3$. Scolnic et al. (2022) fitted the light curves with the SALT2 model (Guy et al. 2007) following Brout et al. (2022a). We used the x_0 light-curve amplitudes as $m_B \equiv -2.5 \log_{10}(x_0)$, the x_1 stretch and the c color parameters from their fit data². Following Brout et al. (2022b), who built on Tripp (1998) and Kessler & Scolnic (2017), we inferred the distance moduli of the SNe as:

$$\mu_{\text{SN}} = m_B + \alpha x_1 - \beta c - M_B - \delta_{\text{bias}} + \delta_{\text{host}} \quad (2)$$

where α and β are global nuisance parameters, M_B is the fiducial magnitude of an SN, and δ_{bias} is a correction term accounting for selection biases² (see Brout et al. 2022b and Popovic et al. 2021 for details). $\delta_{\text{host}} \equiv \gamma \tilde{\delta}_{\text{host}}(M_\star)$ corrects for residual correlations between the standardized brightness of an SN and the host-galaxy stellar mass (M_\star), γ is a nuisance parameter, and $\tilde{\delta}_{\text{host}}$ is a function of M_\star defined in Equation (2) of Brout et al. (2022b) and Popovic et al. (2021). The M_\star values for the SN hosts² are presented in Scolnic et al. (2022) and references therein. The distance modulus of a source at redshift z is

$$\mu(z) \equiv 5 \log_{10} \left(\frac{d_L(z)}{10 \text{ pc}} \right) \quad (3)$$

² See Pantheon+ data release at <https://github.com/PantheonPlusSH0ES/DataRelease>.

where d_L is the luminosity distance of the source. For the three coasting cosmologies, d_L is

$$d_L(z) = \frac{c}{H_0} (1+z) \begin{cases} \sinh(\ln(1+z)) & \text{for } k = -1 \\ \ln(1+z) & \text{for } k = 0 \\ |\sin(\ln(1+z))| & \text{for } k = +1 \end{cases} \quad (4)$$

and for the flat Λ CDM model, with $H(z)$ given in Equation (1), it is

$$d_L(z) = c(1+z) \int_0^z \frac{dz'}{H(z')}. \quad (5)$$

We fitted the nuisance parameters α , β , γ , M_B and the cosmological parameters H_0 and $\Omega_{m,0}$ simultaneously using our own MCMC code (Raffai et al. 2024b) minimizing

$$\chi^2 = \Delta \mathbf{D}^T C_{\text{stat+syst}}^{-1} \Delta \mathbf{D} \quad (6)$$

where $\Delta \mathbf{D}$ is the vector of 1701 SN Ia distance-modulus residuals computed as

$$\Delta D_i = \mu_{\text{SN},i} - \mu(z_i). \quad (7)$$

$\mu_{\text{SN},i}$ and $\mu(z_i)$ are the distance moduli for the i th SN calculated using Eqs. (2) and (3), respectively, and $C_{\text{stat+syst}}^{-1}$ is the inverse of the covariance matrix accounting for both statistical and systematic uncertainties² (see Brout et al. 2022b). For z_i , we used the cosmological redshift of the SN host galaxy in the CMB frame, corrected for peculiar velocity (denoted as z_{HD} in Pantheon+²; see Carr et al. 2022).

We can see from Eqs. (2) and (3) that M_B and H_0 are degenerate and cannot be fitted independently. To address this, we followed Brout et al. (2022b) by using the Cepheid-calibrated host-galaxy distance moduli μ_i^{Cepheid} from SHOES (Riess et al. 2022) as external calibrators, replacing $\mu(z_i)$ with μ_i^{Cepheid} in Eq. (7) for the 77 SNe where available. We used the $C_{\text{stat+syst}}$ in Eq. (6) that included the Cepheid host-distance covariance matrix from Riess et al. (2022).

Similarly to Amanullah et al. (2010), Riess et al. (2022), and others, we applied the method of *sigma clipping* in model fitting, i.e., we iteratively removed data points that deviated from the global fits by more than 3σ until no such outliers remained. As shown by, e.g., Kowalski et al. (2008) with simulations, this technique preserves the fit results in the absence of contamination and reduces the impact of any contaminating data. Out of the 1701 SN data points, sigma clipping removed $N = \{17, 18, 24\}$ for the $k = \{-1, 0, +1\}$ coasting models and $N = 15$ for the flat Λ CDM model.

Table 2. Model Fit and Test Results for SN Ia Data

Coasting			
	Flat	Closed	Open
α	$0.144^{+0.004}_{-0.004}$	$0.144^{+0.004}_{-0.004}$	$0.146^{+0.004}_{-0.004}$
β	$2.907^{+0.072}_{-0.072}$	$2.887^{+0.072}_{-0.073}$	$2.949^{+0.072}_{-0.072}$
γ	$0.008^{+0.011}_{-0.011}$	$0.004^{+0.011}_{-0.011}$	$0.011^{+0.011}_{-0.011}$
M_B	$-19.187^{+0.031}_{-0.031}$	$-19.177^{+0.031}_{-0.030}$	$-19.198^{+0.031}_{-0.031}$
H_0	$71.39^{+1.02}_{-1.01}$	$71.02^{+1.01}_{-0.99}$	$71.71^{+1.04}_{-1.02}$
χ^2	1820	1981	1775
$\log_{10} \mathcal{B}$	0.003	0 (1.950)	1.207
Flat Λ CDM			
α		$0.149^{+0.004}_{-0.004}$	
β		$2.979^{+0.070}_{-0.072}$	
γ		$0.010^{+0.011}_{-0.011}$	
M_B		$-19.210^{+0.031}_{-0.031}$	
H_0		$73.13^{+1.08}_{-1.05}$	
$\Omega_{m,0}$		$0.328^{+0.018}_{-0.018}$	
χ^2		1755	
$\log_{10} \mathcal{B}$		2.502	

NOTE— H_0 values are given in [km s⁻¹ Mpc⁻¹] units. $\log_{10} p_{\max}^{-1} = 1.950$ (for the closed coasting model) is shown in brackets in the $\log_{10} \mathcal{B} = \log_{10}(p_{\max}/p)$ row. Plots of posterior distributions are available in our public code repository (Raffai et al. 2024b).

We present the best-fit parameters as the medians of the posteriors, along with their 16th and 84th percentile errors, in Table 2. We give the χ^2 values in Table 2 calculated for all 1701 SN observations. Our best-fit H_0 and $\Omega_{m,0}$ for the flat Λ CDM model are consistent with $H_0 = 73.6 \pm 1.1$ km s⁻¹ Mpc⁻¹ (within 0.3σ) and $\Omega_{m,0} = 0.334 \pm 0.018$ (within 0.2σ) in Brout et al. (2022b). Our H_0 is also consistent with $H_0 = 73.30 \pm 1.04$ km s⁻¹ Mpc⁻¹ (within 0.1σ) and $H_0 = 73.04 \pm 1.04$ km s⁻¹ Mpc⁻¹ (within 0.06σ) in Riess et al. (2022), obtained with and without including high-redshift ($z \in [0.15, 0.8]$) SNe in their analysis, respectively.

Our best-fit $H_0 = 73.13^{+1.08}_{-1.05}$ km s⁻¹ Mpc⁻¹ for the flat Λ CDM model is in 4.8σ tension with the Planck+BAO $H_0 = 67.66 \pm 0.42$ km s⁻¹ Mpc⁻¹ (Aghanim et al. 2020). Although the best-fit H_0 values for the $k = \{-1, 0, +1\}$ coasting models are $\{3.7\sigma, 3.4\sigma, 3.1\sigma\}$ above the Planck+BAO H_0 , we cannot claim that these models necessarily alleviate the tension between the CMB- and SN-based H_0 measurements. Strictly linear coasting models face significant challenges in explaining CMB anisotropies, preventing their fit to CMB data. However, quasi-linear versions

of the $k = \{-1, 0, +1\}$ coasting models, with linear expansion in the $z \leq 2.3$ redshift range of Pantheon+ SNe and Λ CDM-type expansion at earlier times, including the time of recombination, may yield a CMB-based H_0 value similar to that of the Λ CDM model, potentially alleviating the H_0 tension.

We applied the same AD test for model comparison as in Section 2. Since practically none of the 1701 SN data points should deviate from a cosmological model by more than 4σ , we excluded such outliers from the AD-tested samples, assuming non-cosmological contamination. The five excluded data points were the same for all tested models. None of the best-fit models met the $p \geq 0.05$ criterion for consistency with the SN data, with the closest ones being $p = 0.01$ for the closed and flat coasting models ($\log_{10} p_{\max}^{-1} = 1.950$ and $\log_{10} p^{-1} = 1.953$, respectively; see Table 2). The closed and flat coasting models are strongly favored over the open coasting ($\log_{10} \mathcal{B} \simeq 1.2$) and the flat Λ CDM models ($\log_{10} \mathcal{B} \simeq 2.5$). In light of the lower χ^2 values for the flat Λ CDM ($\chi^2 = 1755$) and open coasting ($\chi^2 = 1775$) models than for the flat and closed coasting models ($\chi^2 = 1820$ and $\chi^2 = 1981$, respectively; see Table 2), these preferences suggest that the former two models overfit the SN data. The upper panel of Figure 2 shows the histograms of normalized residuals for the best-fit flat coasting and flat Λ CDM models, with a reference curve for the standard normal distribution expected for the true model underlying the SN data. Low-value residuals are indeed overrepresented in the Λ CDM sample, with the sample standard deviation being $\sigma = 0.95$ compared to $\sigma = 1.00$ for the flat coasting sample. In the lower panel of Figure 2, we present histograms of AD-test $\log_{10} p$ values for half a million realizations of flat Λ CDM and coasting models, sampled from the joint posterior distributions fitted to the 1701 Pantheon+ SN Ia observations. None of the flat Λ CDM realizations satisfy the $p \geq 0.05$ condition for consistency with the Pantheon+ sample, while $\{0\%, 19\%, 23\%\}$ of the open, closed, and flat coasting model realizations do. Additionally, p -values exceed the highest (median) p -value of the flat Λ CDM realizations for $\{25\%, 70\%, 71\%\}$ ($\{84\%, 96\%, 96\%\}$) of open, closed, and flat coasting model realizations, respectively. These results show a clear overall preference for coasting models over the flat Λ CDM model by the Pantheon+ SNIa sample.

The flat Λ CDM model being less favored by the SN data is not due to sigma clipping. Without the iterative outlier rejection, the $k = +1$ coasting model is the most favored by data, with $p = 0.014$. The flat coasting model is only slightly less

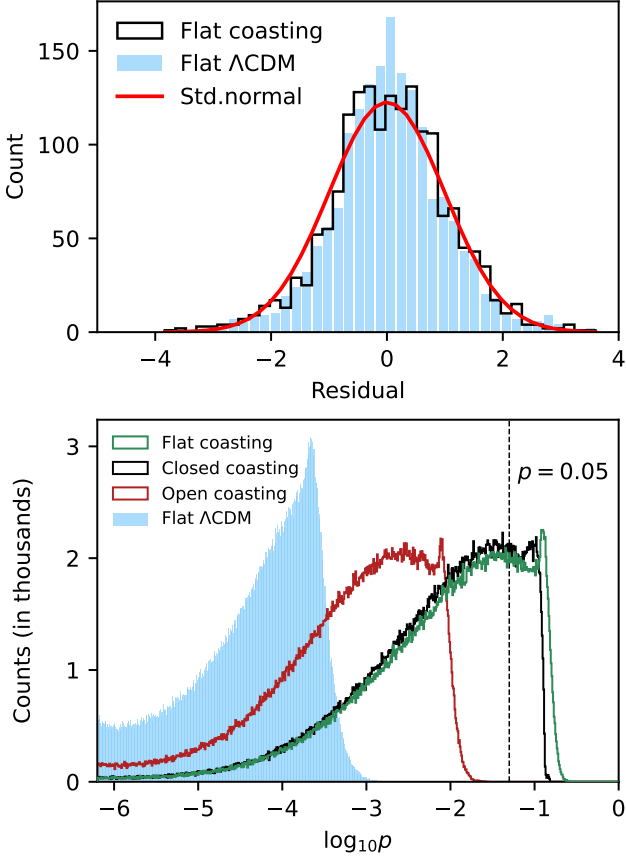


Figure 2. Upper panel: Histograms of normalized residuals for the best-fit flat coasting and flat Λ CDM models, after fitting the Pantheon+ SN Ia data (Scolnic et al. 2022). For both models, we excluded five outliers exceeding 4σ from the 1701 data points. The red curve shows the standard normal distribution expected for the true model underlying the data. Low-value residuals are clearly overrepresented in the Λ CDM sample, with the sample standard deviation being $\sigma = 0.95$ compared to $\sigma = 1.00$ for the flat coasting sample. Lower panel: Histograms of AD-test $\log_{10} p$ values for half a million realizations of flat Λ CDM and coasting models, sampled from the joint posterior distributions obtained from fitting to 1701 Pantheon+ SN Ia observations. Realizations with $p \geq 0.05$ ($\log_{10} p = -1.301$, dashed line) are consistent with the null hypothesis of being the true model: 0% for flat Λ CDM, and {0%, 19%, 23%} for open, closed, and flat coasting models, respectively.

avored ($\log_{10} \mathcal{B} \simeq 0.2$), while the strong preference over the flat Λ CDM ($\log_{10} \mathcal{B} \simeq 2.8$) and open coasting models ($\log_{10} \mathcal{B} \simeq 1.2$) remains. Without sigma clipping, no flat Λ CDM realizations satisfy $p \geq 0.05$, while {0%, 21%, 19%} of open, closed, and flat coasting model realizations do. The highest (median) p -value for flat Λ CDM is exceeded by {42%, 81%, 75%} ({87%, 98%, 96%}) of p -values for open, closed, and flat coasting models, respectively.

To provide broader context for Table 2, we also fitted a coasting model to SN data for which we allowed k to vary freely between -2 and 2 in $H_0^2 c^{-2}$ units. The best-fit k is $k = -1.044^{+0.139}_{-0.140}$, with other parameters and χ^2 differing by no more than 0.06% from those in Table 2 for the open ($k = -1$) coasting model. The model yields $\log_{10} \mathcal{B} = 1.240$, also very close to the $\log_{10} \mathcal{B} = 1.207$ of the open coasting model. We have made the posterior distribution plots available in our public code repository (Raffai et al. 2024b).

4. TESTS WITH QUASARS

The Pantheon+ compilation allows testing cosmologies only up to $z \simeq 2.3$. As Risaliti & Lusso (2015) point out, QSOs can serve as standardizable candles to extend this test to higher redshifts, even as high as $z \simeq 7.54$ (Lusso et al. 2020). QSO standardization is based on the empirical relation $\log(L_X) \propto \log(L_{UV})$ between their rest-frame monochromatic luminosities at 2 keV and 2500 Å (Risaliti & Lusso 2015). This relation allows the QSO distance modulus to be given as

$$\mu_{\text{QSO}} = \frac{5}{2(\gamma - 1)} [\log_{10}(F_X) - \gamma \log_{10}(F_{UV})] - \beta \quad (8)$$

where F_X and F_{UV} are the measured rest-frame fluxes at 2 keV and 2500 Å, respectively, and γ and β are global nuisance parameters (Risaliti & Lusso 2015). These parameters can be calibrated using QSOs with known z , F_X , and F_{UV} values against SNe Ia with known distance moduli (see, e.g., Risaliti & Lusso 2015), or by fitting them alongside the parameters of a cosmological model. We used the latter approach, fitting the coasting and flat Λ CDM models to QSO data from Lusso et al. (2020) with the same MCMC code (Raffai et al. 2024b) as in Section 3. Since a full covariance matrix was not published with the QSO data, we minimized:

$$\chi^2 = \sum_{i=1}^{\text{QSOs}} \frac{[\mu_{\text{QSO},i} - \mu(z_i)]^2}{\sigma_{\mu,i}^2} \quad (9)$$

where $\mu_{\text{QSO},i}$ and $\mu(z_i)$ are the distance moduli for the i th QSO calculated using Eqs. (8) and (3). The variance of $\mu_{\text{QSO},i}$ is:

$$\sigma_{\mu,i}^2 = \frac{25}{4} \frac{\sigma_{X,i} \sigma_{U,i}}{(\gamma - 1)^2} \left(\frac{\sigma_{X,i}}{\sigma_{U,i}} + \gamma^2 \frac{\sigma_{U,i}}{\sigma_{X,i}} - 2\gamma r_{\{X,U\}} \right) \quad (10)$$

where $\sigma_{X,i}$ and $\sigma_{U,i}$ are the errors on $\log_{10}(F_X)$ and $\log_{10}(F_{UV})$, respectively, and $r_{\{X,U\}} = 0.776$ is their sample Pearson correlation coefficient (note that Lusso et al. 2020 ignored the $r_{\{X,U\}}$ term when fitting the same QSO data). We used the symmetrized H_0 posteriors from the SN fits (see Table 2) as priors for the QSO

Table 3. Model Fit Results for QSO Data

Coasting (SNe H_0 posteriors used as H_0 priors)			
	Flat	Closed	Open
γ	$0.707^{+0.002}_{-0.002}$	$0.683^{+0.002}_{-0.002}$	$0.718^{+0.002}_{-0.002}$
β	$56.675^{+0.222}_{-0.224}$	$54.475^{+0.195}_{-0.168}$	$57.789^{+0.209}_{-0.208}$
H_0	$71.38^{+1.01}_{-1.01}$	$71.02^{+0.99}_{-0.99}$	$71.72^{+1.03}_{-1.02}$
χ^2	478603	480589	480789
Flat Λ CDM (SNe H_0 posterior used as H_0 prior)			
γ		$0.709^{+0.002}_{-0.002}$	
β		$56.828^{+0.226}_{-0.220}$	
H_0		$73.14^{+1.05}_{-1.06}$	
$\Omega_{m,0}$		0.328 (fixed)	
χ^2		484056	

NOTE— H_0 values are given in $[\text{km s}^{-1} \text{Mpc}^{-1}]$ units. Plots of posterior distributions are available in our public code repository (Raffai et al. 2024b).

fits. Due to degeneracy between β and H_0 (cf. Equation (9) with Eqs. (8) and (3)), their QSO posteriors are determined by these H_0 priors.

As in Section 3, we applied iterative $> 3\sigma$ outlier rejection (sigma clipping), also used by Bargiacchi et al. (2021) in fitting the same QSO dataset. For the flat Λ CDM model, we fixed $\Omega_{m,0}$ at its SN best-fit value, as the fit did not converge within the physical range $\Omega_{m,0} \in [0, 1]$ when $\Omega_{m,0}$ was left free. Out of the 2421 μ_{QSO} data points, sigma clipping removed $N = \{1573, 1607, 1649\}$ for the $k = \{-1, 0, +1\}$ coasting models and $N = 1606$ for flat Λ CDM, due to large intrinsic scatter. Note that including the covariance term in Equation (10) reduces the $\sigma_{\mu,i}$ errors compared to when it is ignored (e.g., in Lusso et al. 2020), resulting in more outliers being rejected by sigma clipping. Table 3 shows the best-fit parameters for the remaining $\sim 1/3$ of the data, presented as the medians of the posteriors with 16th and 84th percentile errors. The χ^2 values in Table 3 were calculated using Equation (9) and all 2421 data points.

AD test implementations, including the one used in Sections 2 and 3, are unreliable for extremely low p -values, such as those we obtained from the QSO data even after excluding $> 4\sigma$ outliers. However, with $\Omega_{m,0}$ fixed for the flat Λ CDM model, the fitted parameters are the same for all models, and the H_0 priors are also similar in width and shape. We therefore expect the differences in degrees of freedom for the four model fits to be negligible, making the χ^2 values in Table 3 directly applicable for model comparison. Based on these χ^2 values, the QSO data favors the coast-

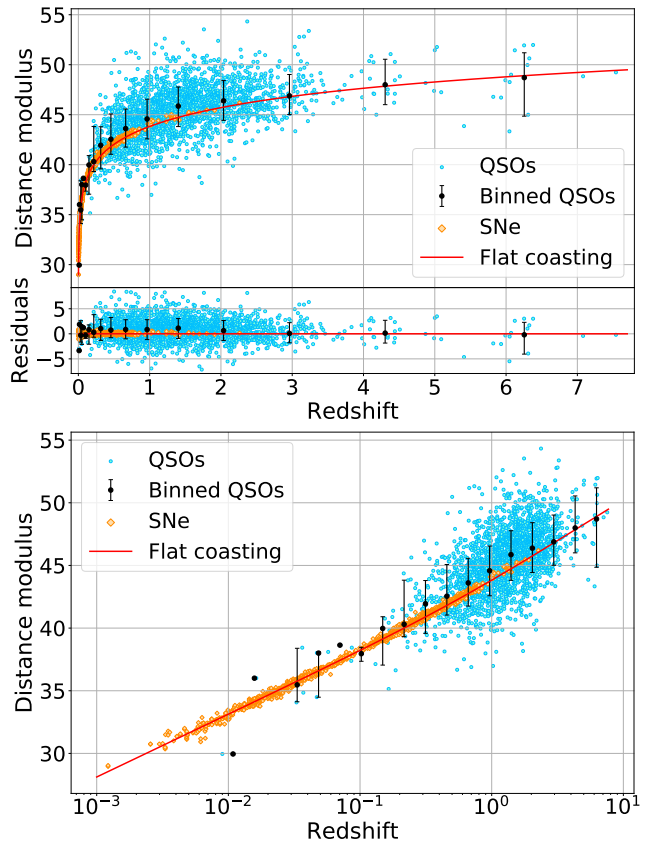


Figure 3. Distance moduli (shown without error bars) for 1701 SN Ia observations (orange diamonds) and 2421 QSOs (blue dots) calibrated to the flat coasting model with $H_0 = 71.39^{+1.02}_{-1.01} \text{ km s}^{-1} \text{Mpc}^{-1}$ (red solid curve; see Sections 3 and 4 for details). Data is from the Pantheon+ sample (Scolnic et al. 2022) and Lusso et al. (2020). The normalized residuals are shown after subtracting the model $\mu(z)$ curve, along with the median μ_{QSO} values in logarithmic redshift bins (black dots with 16th and 84th percentile error bars). These median μ_{QSO} points were not used in the fitting process and are shown only for visualization. The upper and lower panels display the data on linear and logarithmic redshift scales, respectively.

ing models over Λ CDM, with the flat coasting model being the most preferred. As a summary of the results from Sections 3 and 4, Figure 3 shows the distance moduli for Pantheon+ SNe and Lusso et al. (2020) QSOs, calibrated to the best-fit flat coasting model with $H_0 = 71.38 \pm 1.01 \text{ km s}^{-1} \text{Mpc}^{-1}$.

5. CONCLUSION

In Sections 2–4, we presented tests and comparisons of coasting cosmological models with $k = \{-1, 0, +1\}$ in $H_0^2 c^{-2}$ units and the flat Λ CDM model. We carried out the tests by fitting the models to $H(z)$ data derived from CCs (Moresco et al. 2022), and distance moduli

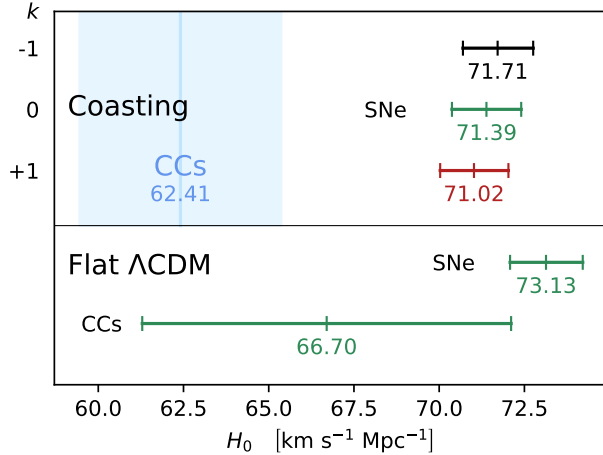


Figure 4. Best-fit H_0 values for coasting models with $k = -1$ (black), $k = 0$ (green), and $k = +1$ (red) in $H_0^2 c^{-2}$ units (upper panel) and for the flat Λ CDM model (lower panel), based on cosmic chronometer (CCs) from Moresco et al. (2022) and type Ia supernova (SNe) data from Scolnic et al. (2022). Best-fit H_0 values based on QSO data from Lusso et al. 2020 are nearly identical to the SNe results (see Table 3) and are thus not shown. The values are the medians of the H_0 posteriors, with 16th and 84th percentile errors shown as error bars. There is a $\sim 3\sigma$ tension between the CC- and SN-based best-fit H_0 values for coasting models, while the Λ CDM model’s H_0 values differ by $\sim 1.2\sigma$.

derived from standardized SNe Ia (Scolnic et al. 2022) and QSOs (Lusso et al. 2020). We used the `emcee`¹ code (Foreman-Mackey et al. 2013) for fitting CC data, our own MCMC implementation (Raffai et al. 2024b) for SNe and QSOs, and AD tests for normality (Anderson & Darling 1952; The MathWorks Inc. 2024) on normalized residuals for model comparisons. To mitigate the effects of non-cosmological contaminations, we applied sigma clipping at 3σ (e.g., Bargiacchi et al. 2021) in our fitting process, and a rejection of $> 4\sigma$ outliers in our AD tests. We carried out the SNe fits using Cepheid-calibrated host-galaxy distance moduli from Riess et al. (2022) as external calibrators. We used the H_0 posteriors of the SN fits as priors for the QSO fits. Results of our fits and tests are summarized primarily in Tables 1–3. We also summarize the best-fit H_0 results for coasting models in Figure 4.

Coasting models are favored over the flat Λ CDM model by all datasets used, with a slight overall preference for the flat ($k = 0$) coasting model. Although none of the best-fit realizations of the four tested cosmological models, including the flat coasting model, met

the $p \geq 0.05$ threshold in AD tests for consistency with the SN and QSO data, 23% of flat coasting model realizations sampled from the joint posterior distribution of parameters satisfied this condition for the SN data (see Section 3). The large intrinsic scatter in μ_{QSO} data, the overfitting of the flat Λ CDM model to Pantheon+SNe, together with the strong explanatory power of the Λ CDM model across other redshift ranges and datasets lead us to conclude that the preference for coasting models indicates a need to refine the error estimations in the SN and QSO data, rather than to revise the concordance cosmological model. At the same time, we highlight the seemingly fine-tuned nature of either the CC data or $\Omega_{\text{m},0}$ in the Λ CDM model to an $H_1 = H_0$ coincidence when fitting $H(z) = H_1 z + H_0$ to CC data (see Section 2 for details), and recommend this for further study.

For the flat coasting model, we suggest using $H_0 = 71.38 \pm 1.01 \text{ km s}^{-1} \text{ Mpc}^{-1}$ (see Table 3) as a baseline for future studies. This value is inferred from four distinct cosmological probes: CCs, SNe Ia, QSOs, and Cepheids as SN calibrators. Note however, that this H_0 value shows a 2.9σ tension with $H_0 = 62.41 \pm 2.96 \text{ km s}^{-1} \text{ Mpc}^{-1}$ inferred from CC data alone (see Table 1). Resolving the tension while preserving the $H_1 = H_0$ coincidence would require the $H(z)$ values from CCs to be systematically higher (or the inferred Δt age differences lower) by $\sim 10\%$.

The baseline H_0 implies an age of the universe of $T = H_0^{-1} = 13.708 \pm 0.194 \text{ Gyr}$ in a strictly linear flat coasting model. However, our tests allow the flat coasting model to be quasi-linear, transitioning from a Λ CDM-like expansion to coasting at redshift z_t between $z_{\text{QSO}}^{\text{max}} \simeq 7.54$ (the redshift of the most distant QSO in Lusso et al. 2020) and $z_* \simeq 1090$ (the redshift at recombination; Aghanim et al. 2020). In this scenario, with $H_0 = 71.38 \text{ km s}^{-1} \text{ Mpc}^{-1}$, the present age of the universe would range from $T_{\text{min}} \simeq 12.27 \text{ Gyr}$ for $z_t = 7.54$ to $T_{\text{max}} \simeq 13.67 \text{ Gyr}$ for $z_t = 1090$.

¹ The authors would like to thank Bence Bécsy, István Csabai, Attila Csótó, Dominika E. Kis, Dávid A. Ködmön and Mária Pálfi for fruitful discussions throughout the project. This project has received funding from the HUN-REN Hungarian Research Network and was also supported by the NKFIH excellence grant TKP2021-NKTA-64.

REFERENCES

- Aasi, J., et al. 2015, *Classical and Quantum Gravity*, 32, 074001, doi: 10.1088/0264-9381/32/7/074001
- Abbott, R., et al. 2023a, *Physical Review X*, 13, 041039, doi: 10.1103/PhysRevX.13.041039

- . 2023b, *ApJ*, 949, 76, doi: [10.3847/1538-4357/ac74bb](https://doi.org/10.3847/1538-4357/ac74bb)
- Acernese, F., et al. 2015, *Classical and Quantum Gravity*, 32, 024001, doi: [10.1088/0264-9381/32/2/024001](https://doi.org/10.1088/0264-9381/32/2/024001)
- Aghanim, N., et al. 2020, *Astronomy & Astrophysics*, 641, A6, doi: [10.1051/0004-6361/201833910](https://doi.org/10.1051/0004-6361/201833910)
- Akutsu, T., Ando, M., Arai, K., et al. 2021, *Progress of Theoretical and Experimental Physics*, 2021, 05A101, doi: [10.1093/ptep/ptaa125](https://doi.org/10.1093/ptep/ptaa125)
- Amanullah, R., Lidman, C., Rubin, D., et al. 2010, *ApJ*, 716, 712, doi: [10.1088/0004-637X/716/1/712](https://doi.org/10.1088/0004-637X/716/1/712)
- Anderson, T. W., & Darling, D. A. 1952, *Annals of Mathematical Statistics*, 23, 193, doi: [10.1214/aoms/1177729437](https://doi.org/10.1214/aoms/1177729437)
- Andrae, R., Schulze-Hartung, T., & Melchior, P. 2010, arXiv e-prints, arXiv:1012.3754, doi: [10.48550/arXiv.1012.3754](https://doi.org/10.48550/arXiv.1012.3754)
- Bargiacchi, G., Risaliti, G., Benetti, M., et al. 2021, *A&A*, 649, A65, doi: [10.1051/0004-6361/202140386](https://doi.org/10.1051/0004-6361/202140386)
- Baumann, D. 2009, arXiv e-prints, arXiv:0907.5424, doi: [10.48550/arXiv.0907.5424](https://doi.org/10.48550/arXiv.0907.5424)
- Borghini, N., Moresco, M., & Cimatti, A. 2022, *ApJL*, 928, L4, doi: [10.3847/2041-8213/ac3fb2](https://doi.org/10.3847/2041-8213/ac3fb2)
- Brout, D., Taylor, G., Scolnic, D., et al. 2022a, *ApJ*, 938, 111, doi: [10.3847/1538-4357/ac8bcc](https://doi.org/10.3847/1538-4357/ac8bcc)
- Brout, D., Scolnic, D., Popovic, B., et al. 2022b, *ApJ*, 938, 110, doi: [10.3847/1538-4357/ac8e04](https://doi.org/10.3847/1538-4357/ac8e04)
- Carr, A., Davis, T. M., Scolnic, D., et al. 2022, *PASA*, 39, e046, doi: [10.1017/pasa.2022.41](https://doi.org/10.1017/pasa.2022.41)
- Casado, J. 2020, *Astrophysics and Space Science*, 365, 16, doi: [10.1007/s10509-019-3720-z](https://doi.org/10.1007/s10509-019-3720-z)
- Di Valentino, E., et al. 2021, *Astroparticle Physics*, 131, 102604, doi: [10.1016/j.astropartphys.2021.102604](https://doi.org/10.1016/j.astropartphys.2021.102604)
- Dodelson, S. 2003, *Modern Cosmology* (Academic Press, Amsterdam)
- Foreman-Mackey, D., Hogg, D. W., Lang, D., & Goodman, J. 2013, *PASP*, 125, 306, doi: [10.1086/670067](https://doi.org/10.1086/670067)
- Fujii, H. 2020, *Research Notes of the American Astronomical Society*, 4, 72, doi: [10.3847/2515-5172/ab9537](https://doi.org/10.3847/2515-5172/ab9537)
- Guth, A. H. 1981, *PhRvD*, 23, 347, doi: [10.1103/PhysRevD.23.347](https://doi.org/10.1103/PhysRevD.23.347)
- Guy, J., Astier, P., Baumont, S., et al. 2007, *A&A*, 466, 11, doi: [10.1051/0004-6361:20066930](https://doi.org/10.1051/0004-6361:20066930)
- Holz, D. E., & Hughes, S. A. 2005, *ApJ*, 629, 15, doi: [10.1086/431341](https://doi.org/10.1086/431341)
- Jimenez, R., & Loeb, A. 2002, *ApJ*, 573, 37, doi: [10.1086/340549](https://doi.org/10.1086/340549)
- John, M. V., & Joseph, K. B. 1996, *Physics Letters B*, 387, 466, doi: [10.1016/0370-2693\(96\)01073-8](https://doi.org/10.1016/0370-2693(96)01073-8)
- . 2000, *PhRvD*, 61, 087304, doi: [10.1103/PhysRevD.61.087304](https://doi.org/10.1103/PhysRevD.61.087304)
- . 2023, arXiv e-prints, arXiv:2306.04577, doi: [10.48550/arXiv.2306.04577](https://doi.org/10.48550/arXiv.2306.04577)
- Kaplinghat, M., Steigman, G., Tkachev, I., & Walker, T. P. 1999, *PhRvD*, 59, 043514, doi: [10.1103/PhysRevD.59.043514](https://doi.org/10.1103/PhysRevD.59.043514)
- Kaplinghat, M., Steigman, G., & Walker, T. P. 2000, *PhRvD*, 61, 103507, doi: [10.1103/PhysRevD.61.103507](https://doi.org/10.1103/PhysRevD.61.103507)
- Kessler, R., & Scolnic, D. 2017, *ApJ*, 836, 56, doi: [10.3847/1538-4357/836/1/56](https://doi.org/10.3847/1538-4357/836/1/56)
- Kolb, E. W. 1989, *ApJ*, 344, 543, doi: [10.1086/167825](https://doi.org/10.1086/167825)
- Kowalski, M., Rubin, D., Aldering, G., et al. 2008, *ApJ*, 686, 749, doi: [10.1086/589937](https://doi.org/10.1086/589937)
- Lewis, G. F., Barnes, L. A., & Kaushik, R. 2016, *MNRAS*, 460, 291, doi: [10.1093/mnras/stw1003](https://doi.org/10.1093/mnras/stw1003)
- Lusso, E., et al. 2020, *Astronomy & Astrophysics*, 642, A150, doi: [10.1051/0004-6361/202038899](https://doi.org/10.1051/0004-6361/202038899)
- Melia, F. 2007, *MNRAS*, 382, 1917, doi: [10.1111/j.1365-2966.2007.12499.x](https://doi.org/10.1111/j.1365-2966.2007.12499.x)
- . 2018, *MNRAS*, 481, 4855, doi: [10.1093/mnras/sty2596](https://doi.org/10.1093/mnras/sty2596)
- . 2020a, *The Cosmic Spacetime* (CRC Press, Boca Raton)
- . 2020b, *European Physical Journal Plus*, 135, 511, doi: [10.1140/epjp/s13360-020-00533-2](https://doi.org/10.1140/epjp/s13360-020-00533-2)
- . 2022, *ApJ*, 941, 178, doi: [10.3847/1538-4357/aca412](https://doi.org/10.3847/1538-4357/aca412)
- Melia, F., & Maier, R. S. 2013, *Monthly Notices of the Royal Astronomical Society*, 432, 2669, doi: [10.1093/mnras/stt596](https://doi.org/10.1093/mnras/stt596)
- Melia, F., & Shevchuk, A. S. H. 2012, *Monthly Notices of the Royal Astronomical Society*, 419, 2579, doi: [10.1111/j.1365-2966.2011.19906.x](https://doi.org/10.1111/j.1365-2966.2011.19906.x)
- Milne, E. A. 1935, *Relativity, gravitation and world-structure* (The Clarendon Press, Oxford)
- Monjo, R. 2017, *PhRvD*, 96, 103505, doi: [10.1103/PhysRevD.96.103505](https://doi.org/10.1103/PhysRevD.96.103505)
- . 2024, *ApJ*, 967, 66, doi: [10.3847/1538-4357/ad3df7](https://doi.org/10.3847/1538-4357/ad3df7)
- Moresco, M. 2015, *MNRAS*, 450, L16, doi: [10.1093/mnrasl/slv037](https://doi.org/10.1093/mnrasl/slv037)
- Moresco, M., Cimatti, A., Jimenez, R., et al. 2012, *JCAP*, 2012, 006, doi: [10.1088/1475-7516/2012/08/006](https://doi.org/10.1088/1475-7516/2012/08/006)
- Moresco, M., Pozzetti, L., Cimatti, A., et al. 2016, *JCAP*, 2016, 014, doi: [10.1088/1475-7516/2016/05/014](https://doi.org/10.1088/1475-7516/2016/05/014)
- Moresco, M., Amati, L., Amendola, L., et al. 2022, *Living Reviews in Relativity*, 25, 6, doi: [10.1007/s41114-022-00040-z](https://doi.org/10.1007/s41114-022-00040-z)
- Peebles, P. J., & Ratra, B. 2003, *Reviews of Modern Physics*, 75, 559, doi: [10.1103/RevModPhys.75.559](https://doi.org/10.1103/RevModPhys.75.559)
- Perivolaropoulos, L., & Skara, F. 2022, *NewAR*, 95, 101659, doi: [10.1016/j.newar.2022.101659](https://doi.org/10.1016/j.newar.2022.101659)

- Popovic, B., Brout, D., Kessler, R., Scolnic, D., & Lu, L. 2021, *ApJ*, 913, 49, doi: [10.3847/1538-4357/abf14f](https://doi.org/10.3847/1538-4357/abf14f)
- Raffai, P., Pálfi, M., Dály, G., & Gray, R. 2024a, *ApJ*, 961, 17, doi: [10.3847/1538-4357/ad1035](https://doi.org/10.3847/1538-4357/ad1035)
- Raffai, P., Pataki, A., Böttger, R. L., Karsai, A., & Dály, G. 2024b, Code repository, 1.0, Zenodo, doi: [10.5281/zenodo.14184660](https://doi.org/10.5281/zenodo.14184660)
- Ratsimbazafy, A. L., Loubser, S. I., Crawford, S. M., et al. 2017, *MNRAS*, 467, 3239, doi: [10.1093/mnras/stx301](https://doi.org/10.1093/mnras/stx301)
- Riess, A. G. 2020, *Nature Reviews Physics*, 2, 10, doi: [10.1038/s42254-019-0137-0](https://doi.org/10.1038/s42254-019-0137-0)
- Riess, A. G., Yuan, W., Macri, L. M., et al. 2022, *ApJL*, 934, L7, doi: [10.3847/2041-8213/ac5c5b](https://doi.org/10.3847/2041-8213/ac5c5b)
- Risaliti, G., & Lusso, E. 2015, *ApJ*, 815, 33, doi: [10.1088/0004-637X/815/1/33](https://doi.org/10.1088/0004-637X/815/1/33)
- Scolnic, D., Brout, D., Carr, A., et al. 2022, *ApJ*, 938, 113, doi: [10.3847/1538-4357/ac8b7a](https://doi.org/10.3847/1538-4357/ac8b7a)
- Sethi, M., Batra, A., & Lohiya, D. 1999, *PhRvD*, 60, 108301, doi: [10.1103/PhysRevD.60.108301](https://doi.org/10.1103/PhysRevD.60.108301)
- Simon, J., Verde, L., & Jimenez, R. 2005a, *PhRvD*, 71, 123001, doi: [10.1103/PhysRevD.71.123001](https://doi.org/10.1103/PhysRevD.71.123001)
- . 2005b, *PhRvD*, 71, 123001, doi: [10.1103/PhysRevD.71.123001](https://doi.org/10.1103/PhysRevD.71.123001)
- Stern, D., Jimenez, R., Verde, L., Stanford, S. A., & Kamionkowski, M. 2010, *ApJS*, 188, 280, doi: [10.1088/0067-0049/188/1/280](https://doi.org/10.1088/0067-0049/188/1/280)
- The MathWorks Inc. 2024, adtest, MATLAB Version: 24.1.0.2628055 (R2024a) Update 4, Natick, Massachusetts, United States: The MathWorks Inc. <https://www.mathworks.com/help/stats/adtest.html>
- Tripp, R. 1998, *A&A*, 331, 815
- Zhang, C., Zhang, H., Yuan, S., et al. 2014, *Research in Astronomy and Astrophysics*, 14, 1221, doi: [10.1088/1674-4527/14/10/002](https://doi.org/10.1088/1674-4527/14/10/002)